The Ray Equation Based Checking of the Ultrasonic Reconstruction from Projections

Hemzal D.[1], Jiřík R.[2], Jan J.[2]
[1]Masaryk University, Brno,[2]Brno University of Technology
jan@feec.vutbr.cz

Abstract. Based on strict physical background, we present in this contribution a practically applicable method that can be used to improve the quality of 3D reconstructucted ultrasonic images by refraining from the linear propagation paths of the ultrasonic rays exclusively used in applications so far. Beside this main result, an estimate of the error that is introduced by using the straight rays is given.

1 Introduction

In transmissive ultrasonic computed tomography (USCT), a high number of transducers (transmitting and/or receiving) surrounding the imaged object provide huge amount of data based on received signals, from which the 3D internal structure of the object is to be reconstructed. In such setups, many different types of measurement can be performed: speed of sound (SOS) measurements [1] based on time of the flight (TOF) of the signals, attenuation mapping [2] and Doppler measurements [3] among others.

Of our interest is the SOS mapping [4]. The so far used reconstruction methods are, basically, using the straight-ray approximation of the ultrasound propagation, which is obviously rather rough. This contribution aims at improving the reconstructions by introducing a physically based higher order model of ultrasound propagation (here however, in contrast to direct forward simulation, [5]-[8], chosen as simple as possible in order to keep the reconstruction efforts reasonable).

Fig. 1: The USCT experimental setup as developed in KIT, Germany. a) the tank with protrusions to be sealed by individual TASes, b) a TAS.

The experimental setup of a 3D USCT system is being developed [9] at Karslruhe Institute of Technology (KIT), Germany (see Fig. 1). The model that we use is the generation I type, with cylindrical tank of 180 mm diameter and height of 140 mm. The tank is equipped with 3 rotatable rings containing 16 transducer arrays (TASes) each. Every TAS consists of 8 groups, each group having a square configuration of 1 sender (in the centre) and 4 receivers (in the corners). In this way, 384 senders and 1536 receivers are present. The rings can be turned an fixed in six different positions, giving a maximum number of 3 538 944 sender-receiver combinations for the measurement.

For a sample with known configuration we can construct a precise geometrical model of the acquisition setup and obtain the rays (in contrast to full direct simulation of the US field, using a Zoeppritz-type equivalent [10] of Snell's law is usually sufficient for simple configurations), see Fig 2. Such a model yields in both a qualitative and quantitative ways - in shape as well as

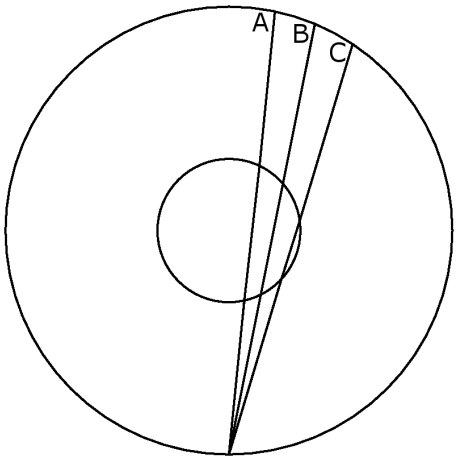

Fig. 2: The geometrical model for the simulated configuration with three selected rays. The outer ring has diameter of 180 mm, the inner one of 64 mm; for further details see below.

in the TOF - the difference between the true rays and the straight ones ususally considered in projections.

Ray	**TOF, true ray**	**TOF, straight ray**	**difference**
A	0.119060 ms	0.119919 ms	0.859 μs
B	0.117401 ms	0.118144 ms	0.743 μs
C	0.114875 ms	0.115396 ms	0.521 μs

Tab. 1: TOF for true and straight rays in geometrical configuration

In Tab. 1 the values for TOF are given for several rays of a chosen geometry. Note that the differences in TOF are markable - with real USCT sampling frequency of 10 MHz it gives up to more than 8 samples difference in TOF. The correction to true rays is, hence, of prime interest if we want to reach the subwavelength resolution needed for tomographic imaging. Otherwise these errors will contribute significantly to overall image blurring during reconstruction.

2 Methods

Concerning the values of action S for individual physical systems, the variational principle can be in the case of rays in general medium shown to require the path integral

$$\int n \mathrm{d}s$$

to take stationary values, bringing thus Fermat's principle in terms of extremal optical path $n\mathrm{d}s$ into action. The ratio $n = c/v$ of the two (phase) speeds of propagation of the waves is the index of refraction with c being the speed in some reference medium (e.g. for light, vacuum is usually taken as a reference). Note that $n(\vec{x})$ is generally not a constant as the speed of propagation v in the selected (possibly nonhomogeneous) medium changes from place to place.

It can be shown, that the integral formulation above has a differential equivalent, namely the differential equation of rays [11],

$$\frac{\mathrm{d}}{\mathrm{d}s}\left(n\frac{\mathrm{d}\vec{x}}{\mathrm{d}s}\right) = \vec{\nabla} n. \tag{1}$$

Realizing that $n\mathrm{d}s = c\mathrm{d}t$ we can write the last equation in a slightly different form,

$$\frac{\mathrm{d}}{\mathrm{d}t}\left(\frac{1}{v^2}\frac{\mathrm{d}\vec{x}}{\mathrm{d}t}\right) = -\frac{\vec{\nabla}v}{v}, \tag{2}$$

which is directly usable for the ultrasound propagation calculations, if treated correctly: although the speed $v(t)$ is of course just the magnitude of the local velocity $|\mathrm{d}\vec{x}/\mathrm{d}t|$ of the waves, in (2), $v(\vec{x})$ must be treated as a given external quantity (coming from the SOS measurements), which will determine the unknown components of the velocity vector $\vec{v} \equiv \mathrm{d}\vec{x}/\mathrm{d}t$. This attitude is mathematically justified by the fact, that knowing the measured distribution of speed $v(\vec{x})$ gives by itself no information on $v(t)$; for this purpose the trajectories $\vec{x}(t)$ are needed, which are obtained only after solving (2).

Carrying out the operations indicated in (2), final equations to be solved are obtained; in our case (of two dimensions), the set

$$\begin{aligned}\frac{\mathrm{d}\dot{x}}{\mathrm{d}t} &= \frac{-v^2\dfrac{\partial v}{\partial x} + 2(\vec{\nabla}v \cdot \dot{\vec{x}})\dot{x}}{v} \\ \frac{\mathrm{d}\dot{y}}{\mathrm{d}t} &= \frac{-v^2\dfrac{\partial v}{\partial y} + 2(\vec{\nabla}v \cdot \dot{\vec{x}})\dot{y}}{v}\end{aligned} \tag{3}$$

evolves the velocity components $\dot{x}$, $\dot{y}$ from their starting values. The consistency must only be preserved by a correct choice of the initial conditions: $\sqrt{\dot{x}^2(0) + \dot{y}^2(0)} = v(x(0), y(0))$ is required. In other words, the magnitude of chosen initial velocity components must coincide in the chosen starting point with the measured speed $v(\vec{x})$ in that point.

For the purpose of verification of the presented method we give below (see Fig. 3) the results of simulation with artificially selected configuration. With regard to size and discrete character of the measured SOS data to be processed we have chosen a map of 22 cm x 22 cm sampled with 128 pixels in each of dimensions (ie. with resolution of approx. 1.64 mm/pixel) with radial distribution of propagation speed, centered within the image with value 1500 m/s and rising linearly with distance towards the edges of the image to maximal value of 2405 m/s (in the corners). The time step of 1 μs was chosen for the simulation with total time simulated of 0.14 ms.

Note in Fig 3, panel b), that the simulated velocity components indeed fulfill the requirement that their magnitude in every instant of time must agree with the input SOS values. This agreement (the step form of the SOS values is given by the chosen SOS map resolution) was reached by only setting these components properly in the first step of integration, as described above.

3 Results

The procedure suggested here consists in calculating the best possible classical reconstruction [12] (possibly with synthetic aperture focusing on the sides of both sender and receiver by combining more transducers) adopted with suitable regularization [13] followed by the calculation of the rays for this SOS map according to eq. (3), see Fig. 4. Subsequently, one can directly compare the differences of this solution to the one for true rays from the geometrical model of the acquisition system (see Tab. 1). In addition, the straight rays TOF can be computed from the SOS map, [14].

In the real measurement carried out with the USCT equipment a gelatine phantom of 64 mm diameter submerged in water was used. The temperature of water during measurement was 23.5 °C to 24.1 °C, bringing theoretical speeds of ultrasoundsound of 1492.6 m/s to 1494.3 m/s. As for the phantom, 60 g of gelatine was used for 0.5 l of water (50 g of gelatine for 0.5 l water

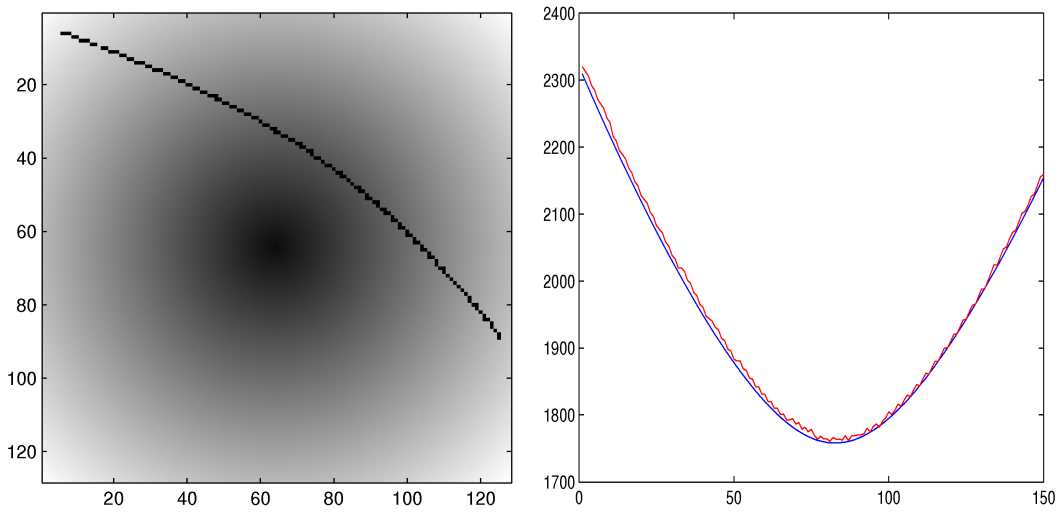

Fig. 3: The results for simulation of ray propagation in artificial configuration. a) the speed of propagation ranging from 1500 m/s to 2405 m/s; the pixels hit by simulated ray are marked. b) a comparison of calculated propagation speed (blue) to input SOS data (red).

gives theoraetical speed of propagation 1530 m/s). The configuration was measured and the SOS map was reconstructed over grid of 64 x 64 pixels using the straight rays approximation as usual. For the results of the subsequent direct simulation, see Fig. 4; the ray depicted is the B ray from Fig. 2.

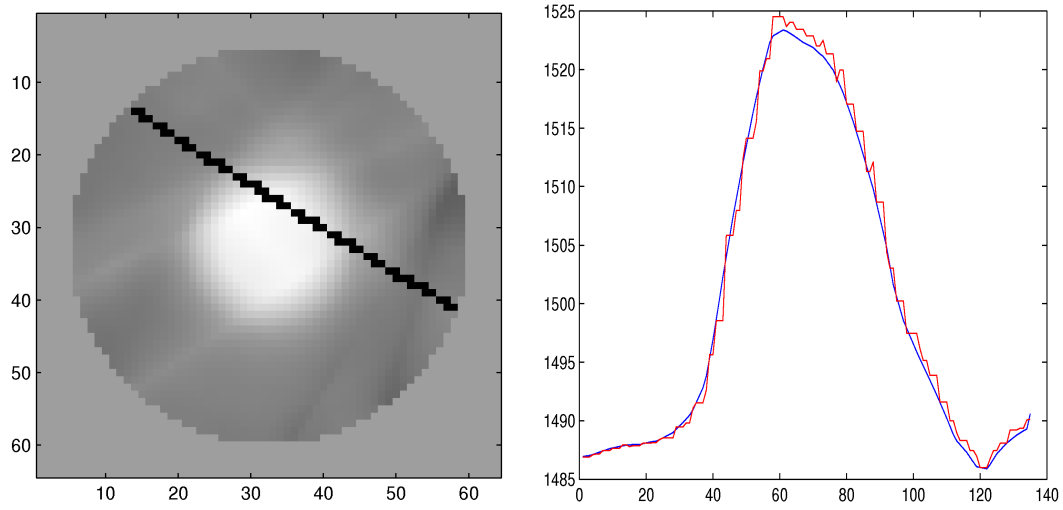

Fig. 4: The results for real phantom simulation of ray propagation. a) the reconstructed SOS map with the pixels hit by simulated ray are marked. b) calculated propagation speed along the simulated ray (blue); again, with input SOS data check (red).

A comparison of the length and TOF of true rays, eq. (3), and straight rays, both calculated from this SOS map, are given in Tab. 2.

The presented method gives us also a readable estimate of the error, that is introduced by using of straight rays during reconstruction. Looking to the Tab. 1, there is approximately 0.75 μs of average difference between bent and straight rays TOF. Having the speeds of propagations approx. from 1493 m/s to 1530 m/s, this gives the length of 1.12 mm to 1.14 mm for an extra path that the faster rays have covered. More precisely, a mean TOF difference can be calculated from all the rays used in reconstruction. Subsequently, in all points of the reconstructed SOS

quantity	TOF	ray length
true ray	0.11400 ms	171.111 mm
straight ray	0.11405 ms	171.110 mm

Tab. 2: Length and TOF for true and straight rays as calculated from SOS map.

map an error can be prescribed coming from their reconstructed values of speed and average TOF difference. In this way, all structures obtained in the reconstruction can be equipped with error estimate in their positions.

4 Discussion

From the results given in previous sections it can be seen, that the two type of rays calculated from SOS map differ each from other much less than their equivalents in precise geometrical model do. This behavior, potentially surprising at first sight, has, however, a good explanation. The problem of the SOS map is the low resolution achievable by current reconstruction algorithms to remain computationally feasible. As a result, the SOS map is smeared in a very smooth manner. The rays in simulation, hence, do not pass sharp edges and have thus no reason to deviate significantly from the stright tajectories. On the other hand, the precise geometrical model (which is reflecting closely the real experiment conditions) contains steep edges of the index of refraction distrubution and the differences between true and straight rays get much greater.

This confirms that for the improved reconstruction much denser sampling of the calculated volume must be applied in the future. Apart from computational issues during reconstruction (which will be solved by improvement of computer hardware) the great issue in the higher density reconstructions is the regularisation, which must be applied in a heuristic way to balance the contrast improvement and numeric artefact production in the SOS maps.

As the need of regularisation is given by straight rays reconstruction, it can be strongly diminished when using the more proper modelling covering the bent rays as we suggest here. The effect of employing our procedure is thus two-fold: both the resolution can be increased and non-naturaly strong regularisations can be omitted.

Moreover, even if utilising eq. (3) was considered too complicated for the purpose of the direct reconstruction (the projection concept of reconstruction using straight rays avoids the usage of differential equations and remains an algebraic problem), still it can be used both for checking whether premises of the classical reconstruction were valid in a particular case and also, which is of even more importance, for increasing the precision of the reconstruction, by including a step subsequent to the classical treatment. Presently, the reconstruction algorithm based utilising of this idea is being implemented.

5 Conclusions

In the presented contribution we directly and quantitatively deduce the differences both in TOF and in geometrical deviations of the ultrasonic rays trajectories. Based on these results, we provide a lower bound estimate (based on the TOF error) of the blurring of the back-projected image due to the imprecision of the straight rays approximation in classical reconstruction formalism.

Extending our previous work [14], we provide all the steps necessary for judging a particular classical reconstruction acceptability (in sense of sufficiency of the straight-rays approximation) via the TOF error estimate in the SOS map. Furthermore, even for images justly reconstructed using straight rays, it is intended that the results can be used for refining the original resolution of the SOS map. This is of great interest because the improved SOS map would (unlike upon simple resampling) contain new, and in this case even truly physically justified,

information.

Of course, using the true rays can not improve reconstructed images past some level, in our case given by diffraction, especially in places where the ultrasonic field impinges the interfaces at oblique angles. However, the bent rays utilisation that we suggest is only the first step towards full direct simulations, that account even for diffraction. The advantage of the presented attitude in comparison with the extremely demanding full simulations is that one can decide what level of approximation to take with respect to the computational resources available.

Acknowledgement

This work has supported by the MSMT projects 1M0572 (Data-Algorithms-Decission making) and MSM0021630513 of the Czech Republic.

References

[1] M.E. Anderson, M.S. McKeag, G.E. Trahey: The impact of sound speed errors on medical ultrasound imaging, J. Acoust. Soc. Am. 107(6), pp. 3540-3548 (June 2000)

[2] S.A. Goss, L.A. Frizzella, F. Dunna: Ultrasonic absorption and attenuation in mammalian tissues, Ultrasound in Medicine & Biology 5(2), 1979

[3] Y. Takeda: Velocity profile measurement by ultrasound Doppler shift method, International Journal of Heat and Fluid Flow, 7(4), 1986

[4] B.A.J. Angelsen: Ultrasound Imaging - Waves, Signals, and Signal Processing, Vol I, II, Emantec 2000, ISBN 82-995811-0-9

[5] J. Zacal, D. Hemzal, J. Jan, A. Filipik, R. Jirik, R. Kolar: Comparison of Wave-Equation Based versus Measurement Processing Transducer Calibration for Ultrasonic Transmission Tomography. Proc. of 28th Annual International Conference IEEE Engineering in Medicine and Biology Society 2006, New York (USA), Aug. 2006, pp. 2754 - 2757, IEEE: ISBN 14244-0033-3

[6] J. Zacal, D. Hemzal, J. Jan, et al., Simulation Checks in Ultrasonic Computed Tomography, in Proceedings of 29th Annual International Conference IEEE EMBS 2007. Lyon (France): 2007, 731-734, ISBN 1-4244-0788-5

[7] D. Hemzal, I. Peterlik, J. Rolecek, J. Jan, N. Ruiter, R. Jirik: 3D Simulation of Diffraction in Ultrasonic Computed Tomography, in Proc. of the 30th Annual International IEEE EMBS Conference, Vancouver, British Columbia, Canada, August 20-24, 2008, pp. 454 -457, ISBN 978-1-4244-1815-2

[8] D. Hemzal et al: Experimental Simulations of Ultrasonic Filed Time-Developmnet in 3D Ultrasonic Transmission Tomography: 9th International Conference on Information Technology and Applications in Biomedicine, ITAB 2009, Cyprus

[9] R. Stotzka, J. Wurfel, T. O. Muller, H.Gemmeke: Medical imaging by ultrasound computer tomography, in SPIEs Internal Symposium Medical Imaging 2002, 2002, pp. 110-119.

[10] Aki K., Richards P.G: Quantitative Seismology, University Science Books 2002, ISBN 978-1891389634

[11] Born M., Wolf E.: Principles of Optics, Cambridge University Press, ISBN 978-0521639217

[12] Jiřík R., Peterlík I et al, 2009 IEEE International Ultrasonics Symposium, Roma 2009

[13] Peterlík I., Jiřík R. et al: Regularized Image Reconstruction for Ultrasound Attenuation Transmission Tomography. Radioengineering, vol. 12, no. 2, pp. 125-132. ISSN 1210-2512, 2008

[14] Hemzal D. et al: Proc. Inter. conf. Data-Algorithms-Decision Making, Pilsen 2009